IMPROVING THE PHYSICAL UNDERSTANDING OF HYDROACOUSTIC BLOCKAGE: STATISTICAL AND MODEL BASED STUDIES

Zachary M. Upton[1], Joydeep Bhattacharyya[1], Jay J. Pulli[1], Sheila Shah[1], and Michael Collins[2]

BBN Technologies[1] and Naval Research Laboratory[2]

Sponsored by National Nuclear Security Administration
Office of Nonproliferation Research and Engineering
Office of Defense Nuclear Nonproliferation

Contract No. DE-AC03-02SF22560

ABSTRACT

The hydroacoustic network of the International Monitoring System (IMS) is a sparse set of only eleven stations. This network relies on the efficient propagation of acoustic energy in the natural underwater waveguide called the sound fixing and ranging (SOFAR) channel. Sound traveling in the channel that encounters an island or seamount must either diffract, scatter, or be translated into seismic energy. When signals from a source are observed from the opposite side of one of these obstructions, they have likely been affected by all of these processes. In past studies, we have shown that ray-based models with a simple, binary blockage condition (i.e., blocked or not blocked) will not suffice for accurate prediction of blockage (Pulli and Upton, 2001). Recently, we have accumulated a set of over 150 events in the Indian Ocean that allowed for an initial assessment of blockage based on recorded data at Diego Garcia (H08).

U.S. Department of Energy (DOE) researchers at Lawrence Livermore National Laboratory have designed a Hydroacoustic Blockage Analysis Tool (HydroacousticBAT) that combines model predictions from the Hydroacoustic Coverage Assessment Model (HydroCAM) and observations from data. The tool will be used to assess ramifications of blockage on the detection and discrimination capability of the hydroacoustic network.

Our current efforts in understating hydroacoustic blockage are focused on improving HydroCAM's modeling capability and interpolating data observations to advance the HydroacousticBAT. The first step in this effort is to characterize amplitude variations in recorded data across the Indian Ocean. This information is essential both for calibrating hydroacoustic propagation and testing modeling techniques. We will present results from an interactive analysis of the signal and noise amplitudes over the 2 – 100 Hz frequency range.

Secondly, a model of blockage, including the effects of diffraction and acoustic-seismic-acoustic energy conversion at islands is required to ensure that we understand the physical processes that produce amplitude variation with blockage in the recoded data. This study describes the initial implementation of an adiabatic mode parabolic equation (AMPE) model for HydroCAM that accounts for these physical processes. We will present initial modeling results and compare it with observations.

Finally, the sparse geographical coverage of the long-range hydroacoustic paths in this region lends itself readily to the well-established Kriging technique, which uses a statistical framework to robustly interpolate between observed values. We will show preliminary models of amplitude variations across the Indian Ocean region, as a function of frequency, in this presentation.

OBJECTIVES

The primary objective of this work is to improve Air Force Technical Applications Center (AFTAC) and Department of Energy (DOE) understanding of hydroacoustic blockage by advancing the modeling capabilities of the Hydroacoustic Coverage Assessment Model (HydroCAM) and using established extrapolation techniques to provide an empirical prediction of blockage to the DOE Hydroacoustic Blockage Analysis Tool (HydroacousticBAT).

We have designed an interactive method to make frequency-dependent measurements of signal amplitude for each of the events in our 150+ event database at Diego Garcia. These observations allow us to compare data observations to model predictions and to calibrate propagation characteristics around Diego Garcia. To improve the modeling capability of HydroCAM, we have obtained the Adiabatic Mode Parabolic Equation (AMPE) model and evaluated its applicability to the blockage problem. This model includes the effects of diffraction and acoustic to seismic to acoustic conversion. We are adapting this model to the environmental databases and software platform used in HydroCAM. We will use the above observations and Bayesian Kriging techniques to extrapolate empirical amplitude measurements into areas where events of opportunity are not available.

RESEARCH ACCOMPLISHED

Amplitude Measurements

To better understand the effects of blockage, BBN has accumulated an event database in the Indian Ocean of more than 150 events recorded at Diego Garcia. In earlier efforts, we compared these data to ray-based blockage models and demonstrated that binary (blocked or not blocked) prediction of blockage was not appropriate, and that future studies needed to account for diffraction and other physical effects that might allow a signal to be detected after interaction with a seamount or island (Pulli and Upton, 2001). Figure 1 shows the origin locations of the database events, with ray paths (regardless of blockage) to Diego Garcia.

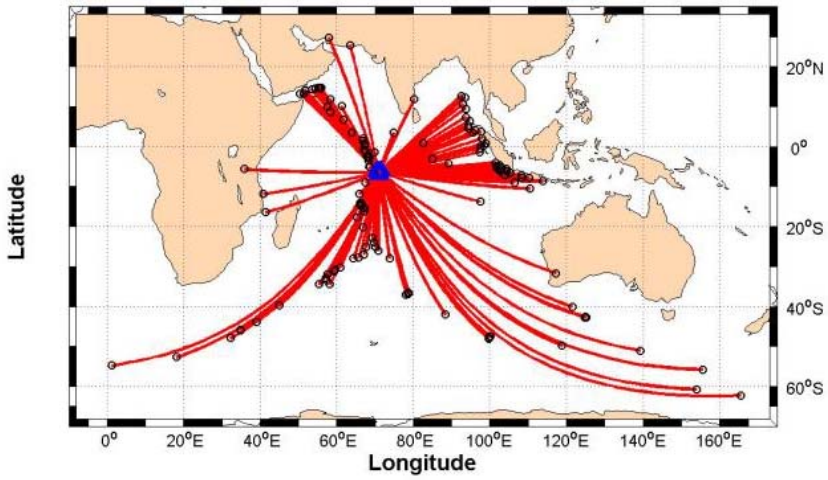

Figure 1. Ray-based blockage predictions for H08N (left) and H08S (right).

In the current study, we are focused on understanding the physical processes of blockage through data analysis and modeling. To gain a uniform set of observations for the ground truth dataset, we have measured the signal and noise levels at the North and South arrays at Diego Garcia. These measurements are valuable in validating models, feeding data extrapolation processes like Kriging, and studying amplitude variations with source magnitude, distance, mechanism, and depth.

To identify the correct earthquake arrival in a signal window, HydroCAM's GlobeRay model (Farrell, et al. 1997) was used to predict acoustic travel time from the event origin to the array at Diego Garcia. This estimate did not

account for the difference in location between earthquake origin and seismic-to-acoustic conversion point, but it was sufficient for identifying the earthquake arrival. Signal and noise level estimates were made for each event in the database by manually picking a signal window and noise window. The signal window was chosen to incorporate the peak (low-order mode) signal energy. The noise window was picked sufficiently far away from signal arrivals to eliminate source effects. An example of the window selection is shown in Figure 2. Both the signal and noise power spectra were computed for both the North and South stations using these chosen windows.

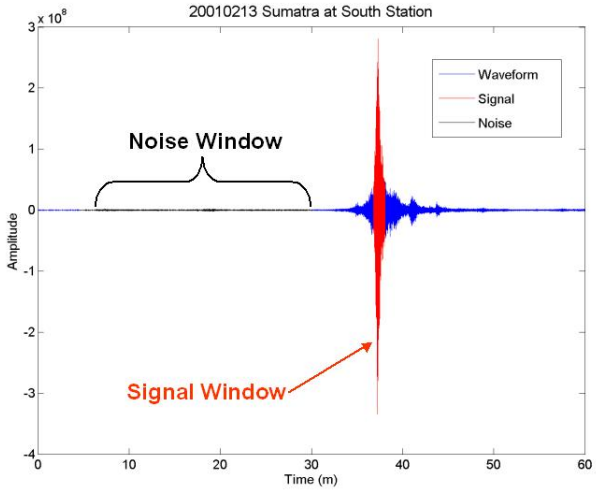

Figure 2. Waveform with signal (red) and noise (black) windows shown after manually choosing them at H08S

One result of these measurements is source and noise spectra. A spectral comparison for the Great Sumatran Earthquake (December 26, 2004, magnitude 9.3) is shown in Figure 3 at 20 Hz. The North station measurement shows a 32 dB difference in signal level over the South station. The difference between the stations for this event is similar to the spectra received from other events in nearby regions of Sumatra.

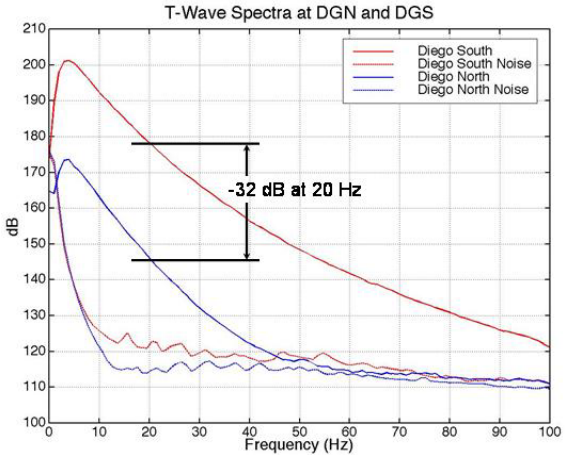

Figure 3. Spectral comparison for the December 26, 2004, Great Sumatran Earthquake recorded at H08N (blue) and H08S (red).

Signal level measurements for the event database are shown in Figure 4 at 20Hz for both the North and South stations (depicted as red triangles). As expected, the signal amplitude detections originating from the Mid Indian Ridge are higher amplitude at the North Station and those originating from Sumatra are higher at the South station. These general results are consistent through a range of frequencies (5Hz–60Hz). Comparison between the stations provides information as to the attenuation of the signals due to the archipelago.

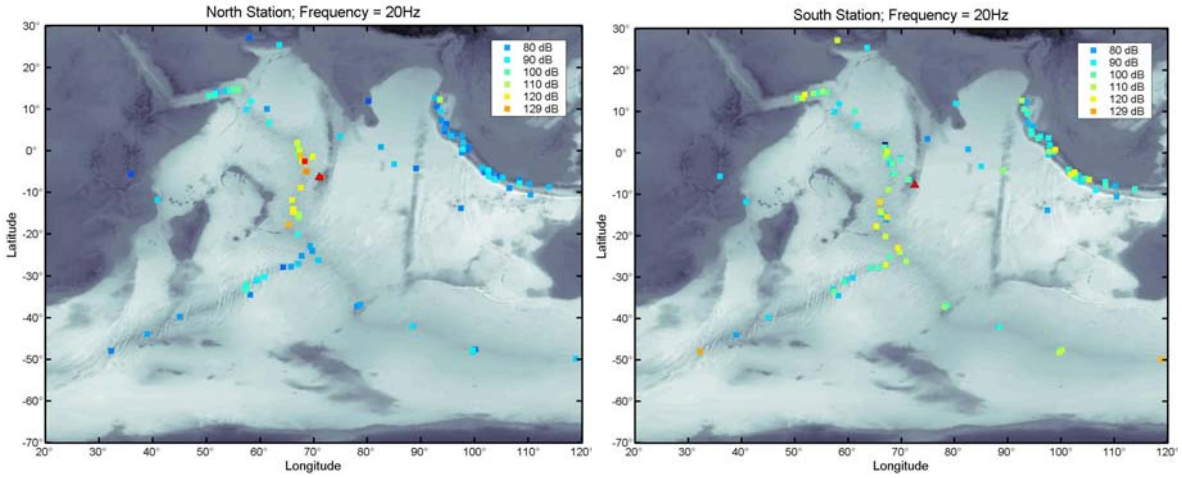

Figure 4. Amplitude estimates at 20Hz for the 150+ events in the ground truth event database at H08N (left) and H08S (right).

In the next few sections, we present analysis of dataset-scale variation in signal amplitudes with frequency, depth and magnitude of the events. The goal of this analysis is to remove some of the source effects from our analysis of blockage.

Frequency Dependence of Signal Amplitudes

We show the large-scale variation of signal and noise with frequency, as recorded at H08N and H08S, in Figure 5. We have combined all of our amplitude measurements in this case, thereby suppressing possible amplitude variations due to changes in signal blockage, source magnitude, source-receiver distance, etc.

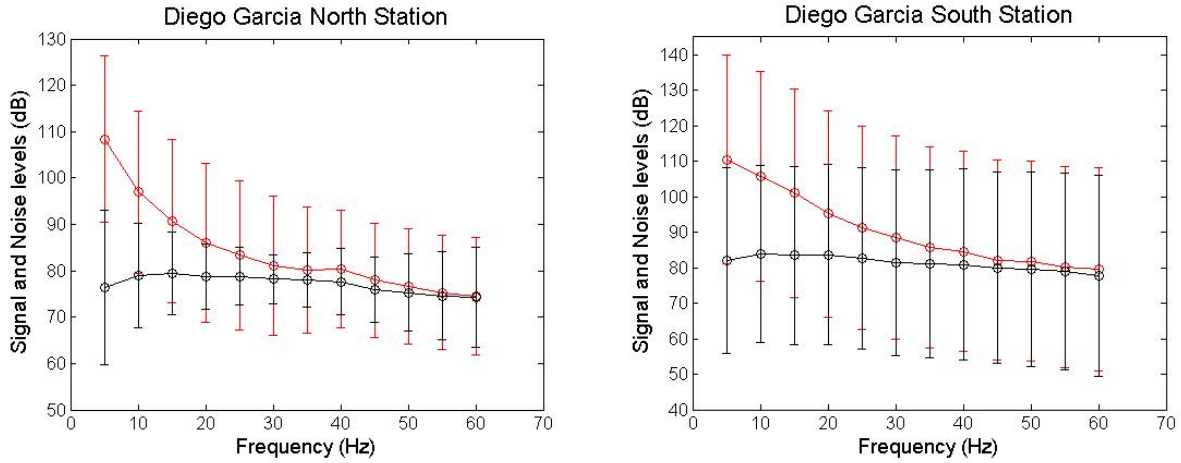

Figure 5. Variation of signal and noise with amplitude for Diego Garcia North and South stations from recorded data. The scatter of the data, shown as the standard deviation of the estimate at each frequency, is shown. It is clear that the signal levels decrease monotonically with frequency while the noise spectra do not show such variations. On average, for our dataset, the signal and noise levels are slightly higher at the South station.

Frequency dependence of SNR

Figure 6 shows a comparison of the large-scale variation of SNR at H08N and H08S. The amplitudes primarily differ within a frequency band of 10-30 Hz.

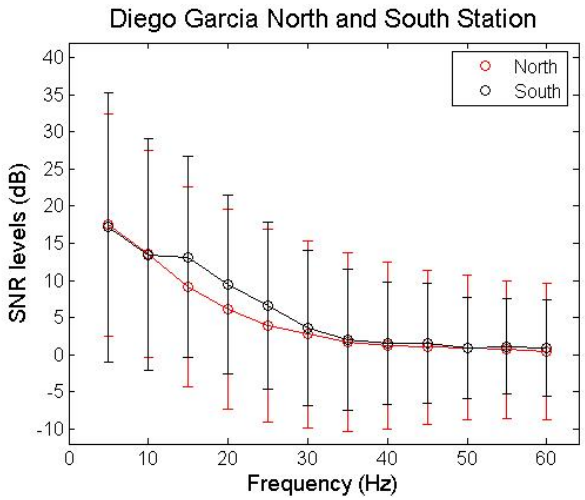

Figure 6. Variation of SNR with frequency for Diego Garcia North (H08N) and South (H08S) arrays for our dataset. On average, the amplitudes differ significantly only within frequencies of 10-30 Hz.

Variation of signal amplitude with event depth

One of the outstanding issues of hydroacoustic propagation is the location of the T-phase conversion region. One of the factors that can affect this location is the depth of the seismic source, as that would control the incidence angle at the crust-water interface. In this section, we investigate the large-scale variation of signal spectra with source depth for events recorded at H08N and H08S. We note that for a significant number of the events in our database, the source depth is known only to a default value, i.e., 10 km or 33 km, depending on the catalog. To decrease the sensitivity of our analysis to such values, we have divided our event into two subsets, deep (depth > 40 km) and shallow. Figure 7 shows the variation of signal amplitude and SNR, with frequency and source depth.

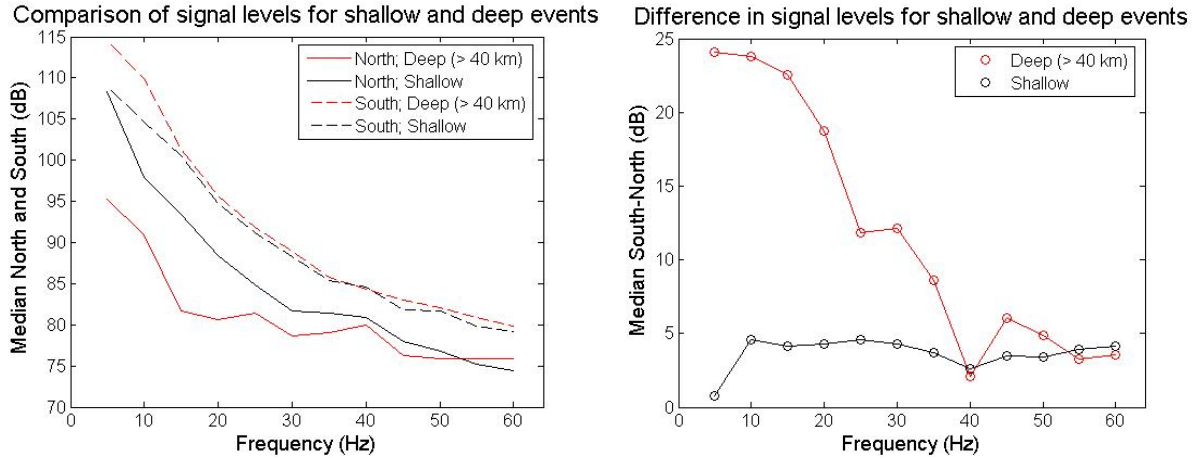

Figure 7. Variation of signal amplitude and SNR with frequency and earthquake source depth. We note that though the event depth does not affect the amplitudes significantly for the southern station (H08S), shallow events have a larger amplitude at H08N up to frequencies of about 35 Hz. The SNR for the deep events is significantly larger at the South station; however, we do not observe this difference for the shallow events. Some of the aforementioned amplitude variations might be accounted for by the differences in typical source depths, sometimes specific to regions, with blocked or unblocked paths.

Variation of signal blockage with frequency

We define blockage as those observations for which the amplitude differs by more than 10 dB between the North and South stations, for a particular frequency. Figure 8 shows the locations of the events for the blocked paths at 20 Hz; a positive value signifies blockage on the North station. We note that the signal is preferentially blocked at the North station from events near Sumatra, the Carlsberg Ridge and the Mid-Indian ridge. Alternately, events located close to the North station are mostly blocked at the South. Next, we separate the paths which are blocked at either the North or the South stations and estimate the variation with frequency.

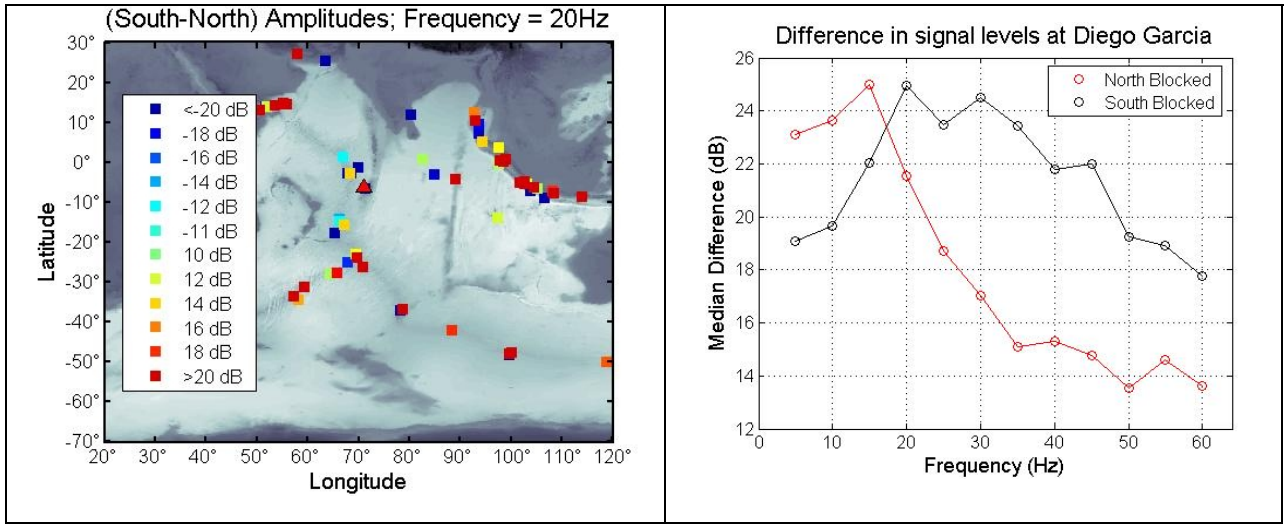

Figure 8. Variation of blocked path with source location (left) and signal frequency. Signals are preferentially blocked at the North station (H08N).

These amplitude measurements will be used to validate new blockage modeling techniques. In addition, we will use these measurements in the Kriging extrapolation process.

Geospatial Analysis of Signal Amplitudes

Robust predictions of amplitudes of hydroacoustic T-phases are essential in nuclear monitoring. In this study, we are augmenting our group's earlier theoretical estimates with measurements from Ground Truth data. These measurements, described above, can be used to map out the spatial variation of the amplitudes recorded at H08N and H08S, as a function of the source locations. However, as is obvious from the map in Figure 1, the geographical distribution of our dataset is inadequate for ocean basin analysis of spatial variation. To use such a sparse dataset to extract robust amplitude predictions, we will use the well-established kriging technique, which allows us to combine the information from our measured and predicted amplitude estimates. Using kriging, we obtain both the amplitude and its formal error on a grid of geographical locations. Using a separate test dataset, we now in turn can evaluate the validity of our kriged model. As an initial analysis step for kriging, here we show the variation of observed amplitude with source-receiver distance, at a set of frequencies (Figure 9).

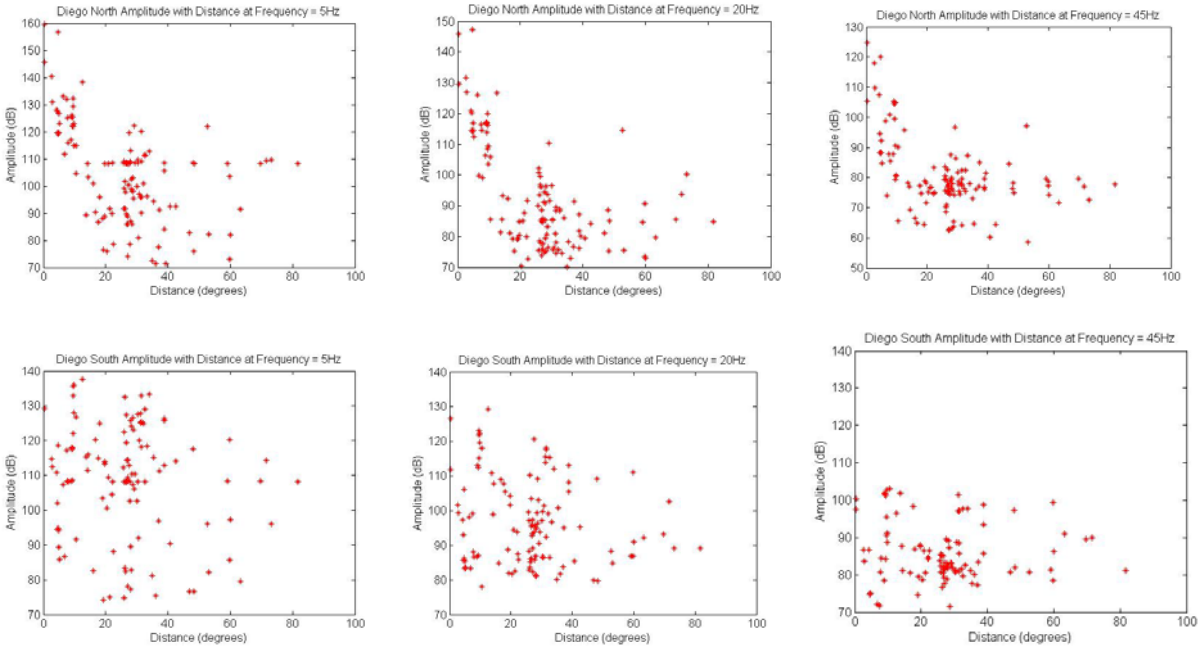

Figure 9. Amplitude distribution with distance and frequency at H08N and H08S.

Blockage Modeling

Prior ray-based modeling did not include the effects of diffraction over and around bathymetric features nor acoustic-seismic-acoustic through the bathymetric feature. The goal of this part of our research is to improve HydroCAM's modeling capability by implementing a model that accounts for the diffraction process. Following a search of published literature, we have obtained the Adiabatic Mode Parabolic Equation (AMPE) model (Collins, 1993) from the Naval Research Laboratory and evaluated its applicability to the blockage problem in nuclear explosion monitoring. The preliminary evaluation of this model is shown here.

The AMPE model merges modal modeling theory with the parabolic equation to predict acoustic propagation in three dimensions in a manner that is efficient for long-range propagation studies in the frequency band of interest for nuclear explosion monitoring (0-150Hz). As the name implies, the model assumes that the environment varies slowly over the horizontal path such that energy does not transfer between modes of the depth-separated wave equation. Each modal coefficient is calculated using the Parabolic Equation (PE) method to solve the acoustic wave equation in latitude and longitude. The model accounts for azimuthal coupling, and therefore horizontal diffraction. (Collins et al., 1995).

Shown here is a model of a source to the East of Diego Garcia, along the same back-azimuth as the origin of the Great Sumatran Earthquake of December 26, 2004. The spectra of that event, recorded at the hydrophones of Diego Garcia, are shown in Figure 3. The output of the AMPE model is in terms of transmission loss (TL), so the difference in TL between the South and North stations at a given frequency should compare directly with the difference in spectral levels between the two tripartites at that same frequency. Figure 10 shows the modeling scenario, plotted on top of the Sandwell and Smith 2-minute bathymetry in the area. Note that there are a number of shallow features along the Chagos Archipelago that could interfere with sound traveling in the SOFAR channel. Figure 11 shows cross sections of bathymetry along straight-line paths from the source location to the centroid of each tripartite. The AMPE model is currently configured to use the DBDB5 5-minute resolution bathymetry, so cross sections are shown for both databases. Note that, for the path to H08N, the DBDB5 bathymetry shows a large subsurface (~100m depth) bathymetric feature along the straight line path, while the Sandwell and Smith bathymetry shows that feature at the surface.

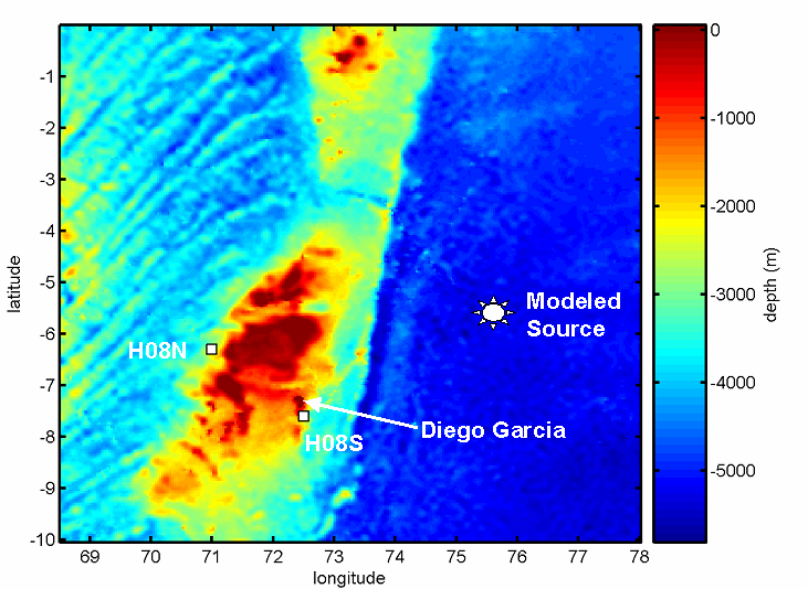

Figure 10. Sandwell and Smith 2-minute resolution bathymetry near Diego Garcia. H08N and H08S station locations are shown as white boxes.

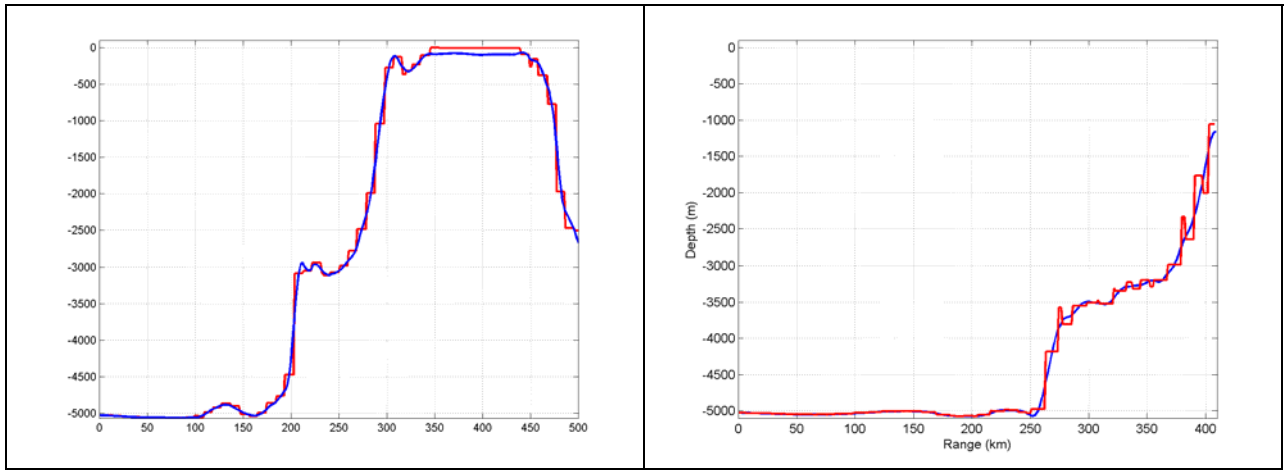

Figure 11. Bathymetric cross sections from the model source location to H08N (right) and H08S (left). DBDB5 data are shown in blue and Sandwell and Smith data are shown in red. Ranges of zero are at the source location while the end of the range axis is the hydrophone location.

Figure 12 shows the output of the AMPE model at 5 Hz. There is a distinct horizontal diffraction pattern around the gross shape of the bathymetry of the Chagos Archipelago. Attenuation between the South and North tripartites is predicted to be over 50 dB, substantially more than the 35 dB shown in Figure 3. In contrast, at 10 Hz, it appears that diffraction over and/or transmission through the features of the archipelago may dominate the propagation prediction. In this case, the approximately 40 dB difference in TL between the two stations is a much closer match to the data shown in Figure 3.

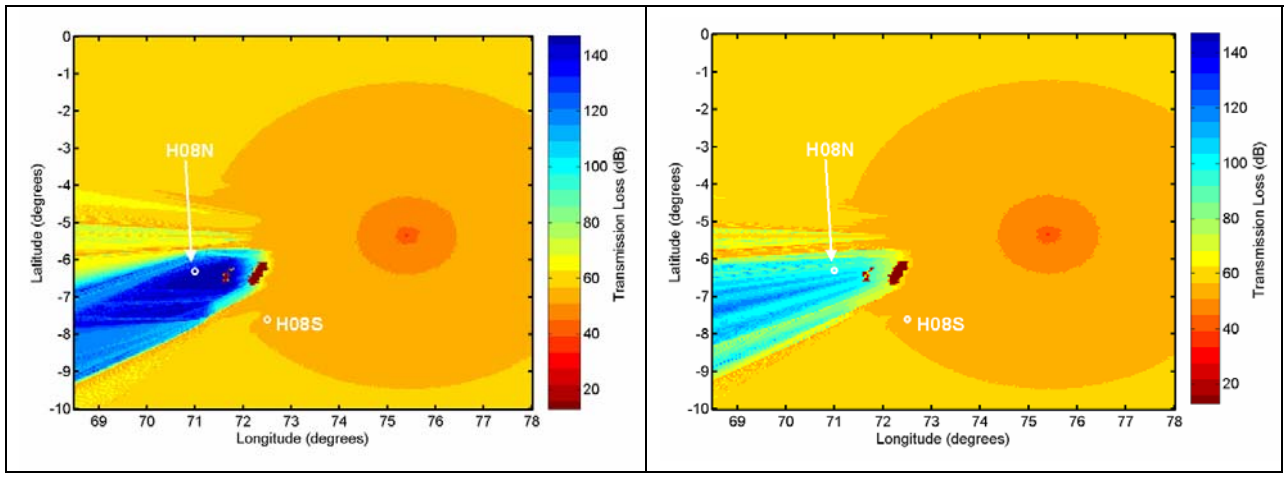

Figure 11. AMPE propagation prediction at 5 Hz (left) and 10 Hz (right).

These preliminary model results will be studied and advanced over the coming months to further understand the output of the AMPE model, the physics of diffraction at the Chagos Archipelago and the use of this model in the context of nuclear explosion monitoring. For example, higher resolution environmental data (bathymetry, sound velocity, etc.) will be integrated into the model. Also, it will be used to predict diffraction and transmission effects from a variety of azimuths. Amplitude measurements will be used to refine and validate the model.

CONCLUSION(S) AND RECOMMENDATIONS

Through a regimen of data analysis and modeling, we are coming to a deeper understanding of the complexity of the blockage issue. For the 150+ earthquake event database, we have measured signal and noise amplitudes and conducted some large-scale analysis to understand source effects on amplitude. Further study is required to completely understand the variation of source amplitudes with event depth, magnitude, azimuth, source mechanism, etc. In the coming months, we will apply Bayesian Kriging techniques to this data in order to predict the spatial effects of bathymetry on signal amplitudes.

We have identified and conducted a preliminary analysis of the (AMPE) model. This model demonstrates potential in the modeling of diffraction and transmission effects on signal amplitude. Initial modeling demonstrates frequency dependence on the physical process of blockage. This model will be integrated into HydroCAM in the next few months. Further study is required to refine the model for nuclear monitoring use, integrate the model into HydroCAM, and thoroughly evaluate the physical process of blockage.

REFERENCES

Bhattacharyya J., A. Rodgers, J. Swenson, C. Schultz, W. Walter, W. Mooney and G. Clitheroe (2000), LLNL's regional model calibration and body-wave discrimination research in the Former Soviet Union using peaceful nuclear weapons (PNEs), in *22nd Annual DoD/DOE Seismic Research Symposium*, Vol. 1, pp. 3-12..

Collins, M. D. (1993), The Adiabatic Mode Parabolic Equation, *J. Acoust. Soc. Am*. 94: (4), pp. 2269-2248

Collins, M. D., B. E. McDonald, K. D. Heaney, and W. A. Kuperman (1995), Three-dimensional effects in global qacoustics. *J. Acoust. Soc. Am*. 97: (3), pp. 1567-1575

Farrell, T., K. LePage, C. Barklay, J. Angell, M. Barger (1997), Users Guide for the Hydroacoustic Coverage Assessment Model (HydroCAM). BBN Technical Memorandum W1309

Fisk, M. S. Bottone, G. McCartor (2000), Regional seismic event characterization using a Bayesiean Kriging Approach, in *22nd Annual DoD/DOE Seismic Research Symposium*, Vol. 1, pp. 23-34.

Pulli, J.J., Z.M. Upton (2001), Hydroacoustic blockage at Diego Garcia: models and observations, in *Proceedings of the 23rd Seismic Research Review: Worldwide Monitoring of Nuclear Explosions*, Vol. 2, pp. 45-54.

Rodgers, A., W. Walter, C. Schultz, S. Myers, and T. Lay (1999), A Comparison of Methodologies for Representing Path Effects on Regional P/S Discriminants, */Bulletin of the Seismological Society of //America/* 89:394-408.